Oxidative and pro-inflammatory effects of cobalt and titanium oxide nanoparticles on aortic and venous endothelial cells

Elsevier Editorial System(tm) for Toxicology in Vitro
Manuscript Draft

Manuscript Number: TIV-D-14-00436R1

Title: Oxidative and Pro-inflammatory Effects of Cobalt and Titanium Oxide Nanoparticles on Aortic and Venous Endothelial Cells

Article Type: Research Paper

Section/Category: Mechanisms

Keywords: Cobalt Oxide Nanoparticles, Titanium Oxide Nanoparticles, Endothelial Cells, Oxidative Stress, Inflammation.

Corresponding Author: Dr. Matteo Goldoni,

Corresponding Author's Institution: University of Parma

First Author: Rossella Alinovi

Order of Authors: Rossella Alinovi; Matteo Goldoni; Silvana Pinelli; Marco Campanini; Irene Aliatis; Danilo Bersani; Pier Paolo Lottici; Sergio Iavicoli; Marta Petyx; Paola Mozzoni; Antonio Mutti

Abstract: Ultra-fine particles have recently been included among the risk factors for the development of endothelium inflammation and atherosclerosis, and cobalt (CoNPs) and titanium oxide nanoparticles (TiNPs) have attracted attention because of their wide range of applications. We investigated their toxicity profiles in two primary endothelial cell lines derived from human aorta (HAECs) and human umbilical vein (HUVECs) by comparing cell viability, oxidative stress, the expression of adhesion molecules and the release of chemokines during NP exposure. Both NPs were very rapidly internalised, and significantly increased adhesion molecule (ICAM-1, VCAM-1, E-selectin) mRNA and protein levels and the release of monocyte chemoattractant protein-1 (MCP-1) and interleukin 8 (IL-8). However, unlike the TiNPs, the CoNPs also induced time- and concentration-dependent metabolic impairment and oxidative stress without any evident signs of cell death or the induction of apoptosis. There were differences between the HAECs and HUVECs in terms of the extent of oxidative stress-related enzyme and vascular adhesion molecule expression, ROS production, and pro-inflammatory cytokine release despite the similar rate of NP internalisation, thus indicating endothelium heterogeneity in response to exogenous stimuli. Our data indicate that NPs can induce endothelial inflammatory responses via various pathways not involving oxidative stress.

Dear TIV Editor,

Herewith we re-submit our manuscript entitled, "Oxidative and Pro-inflammatory Effects of Cobalt and Titanium Oxide Nanoparticles on Aortic and Venous Endothelial Cells".

We thank the referees for their comments, which we have used to improve our manuscript. Our reply to their remarks is enclosed and all the substantial parts modified in the text are in red.

We hope that with this revision the manuscript is now acceptable for publication in Toxicology in Vitro.

Sincerely yours,

Dr. Matteo Goldoni

University of Parma, Italy

Reviewer #1: This paper by Alinovi R, et al. describes oxidative and pro-inflammatory effects of cobalt and titanium oxide nanoparticles on aortic and venous endothelial cells. This is an important and valuable research in nanomedicine and angiology that needs investigating. Thus, some points need clarifying and certain statements require further justification. These are given below.

Reply: we thank the referee for his/her encouraging comments.

General comments

(1) In this study, the used assays covered the study of oxidative and pro-inflammatory effects of cobalt and titanium oxide nanoparticles on aortic and venous endothelial cells. It would be better if some extra data such as ER stress and mitochondrial dysfunction were added.

Reply: this is an important point. As requested by the referee we added our results about Mitochondrial transmenbrane potential and some preliminary data about ER stress measuring the concentration of GRP78. We did not observe any significant effect and it was clearly stated in the manuscript. It should however be noted that ER stress should be studied with a complex battery of tests, which would merit a specific study about it (see for example Chen, R., Huo, L., Shi, X., et al., 2014. Endoplasmic reticulum stress induced by zinc oxide nanoparticles is an earlier biomarker for nanotoxicological evaluation. ACS Nano 8(3), 2562-2574) and it is over the aim of our study.
We include in this response the images of what observed by us, not reported in the manuscript as several figures and tables are already present. We prefer to maintain the original structure of the manuscript.

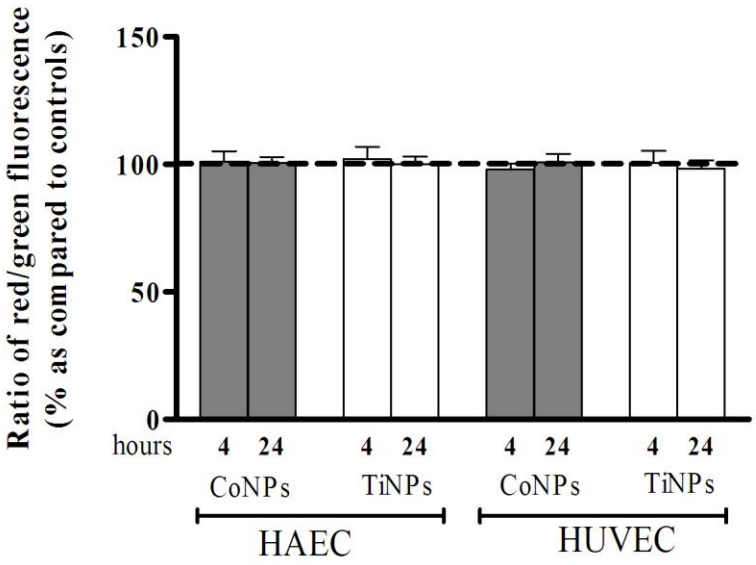

Figure 1: The relative mitochondrial membrane potential was expressed as the ratio of JC-1 red fluorescence to green fluorescence. Flow cytometry confirmed the results (data not shown).

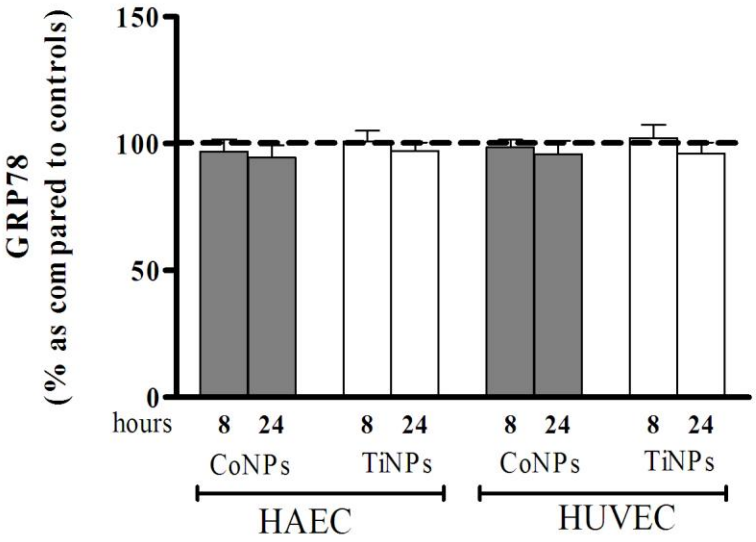

Figure 2: Effect of NPs on GRP78 in HAECs and HUVECs. Values were referred to protein concentrations and expressed as percentage of control.

Additions:

Page 10: methods for Mitochondrial transmenbrane potential and GRP78 enzyme-linked immunosorbent assay. Page 15, results: “No significant differences were observed as compared to

controls looking at mitochondrial transmenbrane potential (NPs 20 μg/ml, 4 and 24 h of exposure, data not shown) and GRP78/BIP levels (NPs 20 μg/ml, 8 and 24 h of exposure, data not shown)."

Discussion, page 18: "However, they also suggest that cells are affected by the presence of NPs even in the absence of evident cellular death and mitochondrial dysfunction". Page 20: a comment about GRP78 role, with the comment: "Although a specific and complete study involving ER stress should be performed (Chen et al., 2014), our preliminary result suggests that ER may be not the main target of NP toxicity".

(2) The authors should comment the differences of HAECs and HUVECs, and the possibility of arteriosclerosis by titanium oxide nanoparticles.

Reply: done in the discussion section, page 21.

(3) The authors should comment the formation of corona in medium with FBS and its effects.

Reply: Page 18, discussion section: "it was expected that albumin may be selectively adsorbed before cell uptake. The presence of 2% foetal bovine serum in the culture medium can complete the protein corona of the studied nanoparticles, but we did not observe any differences in the viability and oxidative stress of HAECs and HUVECs treated with NPs diluted in PBS without BSA (data not shown)."

Reviewer #2: The work by Alinovi et al reports on the oxidative and pro-inflammatory effects in vitro of two different types of nanoparticles on primary cultures of aortic and venous endothelial cells. Authors characterize the physical and aggregation characteristics of Cobalt and Titanium Oxide nanoparticles and apply a battery of cell-based assays to detect cytotoxicity, growth inhibition, oxidative stress and changes in adhesion molecuels and inflammation mediators. The results show the differential cytotoxic and proinflammatory effects of Titanium and Cobalt nanoparticles on the studied cell lines and suggest that nanoparticles may induce toxic and inflammatory effects that may be independent of oxidative stress.

The study is relevant and well performed, but authors have to address some questions before the manuscript is acceptable for publication.

Reply: we thank the referee for his/her encouraging comments.

General Questions:

Manuscript should be thoroughly revised for syntax (e.g the paragraph in lines 34-49 in page 3, Introduction, which is difficult to understand; also, verbal past tens in Material and Methods is used inconsistently) and sparsed mistakes.

Reply: English was completely revised and corrected.

Specific Questions:

Experimental Procedures:

The manufacturer of FC500 flow cytometer is not International Laboratory, but Beckman-Coulter.

Reply: we do agree with the referee. The test was corrected when FC500 is cited.

Regarding the apopotsis assays, authors should indicate clearly if the supernatants of cultures during lavages were kept and mixed with the attached cells for the flow cytometric analysis of apoptosis. Supernatants contain apoptotic cells and if not included in the determination, apoptosis may be underestimated.

Reply: specified at page 9 in the "Apoptosis analysis" sub-paragraph.

The description of cell subpopulations according to the viability state defined by the apoptosis assay might be improved to avoid ambiguity. I suggest the following terminology: Annexin V positive/PI negative cells are considered early apoptotic; Annexin V positive/ PI positive cells are considered late apoptotic/necrotic: Annexin V negative/PI negative cells are considered viable.

Reply: modified at page 9 in the "Apoptosis analysis" sub-paragraph.

Oxidative and Pro-inflammatory Effects of Cobalt and Titanium Oxide Nanoparticles on Aortic and Venous Endothelial Cells.

Rossella Alinovi[1], *Matteo Goldoni*[1]*, *Silvana Pinelli*[1], *Marco Campanini*[2], *Irene Aliatis*[3], *Danilo Bersani*[3], *Pier Paolo Lottici*[3], *Sergio Iavicoli*[5], *Marta Petyx*[5], *Paola Mozzoni*[1,4], *Antonio Mutti*[1]

[1]Department of Clinical and Experimental Medicine, University of Parma, Italy; [2]IMEM-CNR Institute, Parma, Italy; [3]Department of Physics and Earth Sciences, University of Parma, Italy; [4]Italian Workers' Compensation Authority (INAIL) Research Center at the University of Parma, Italy; [5]Italian Workers' Compensation Authority (INAIL), Research Area, Department of Occupational Hygiene, Rome, Italy

Running title: Endothelial cell toxicity of metal oxide nanoparticles.

Corresponding author:

*Matteo Goldoni,

Department of Clinical and Experimental Medicine,

Laboratory of Industrial Toxicology,

University of Parma,

Via Gramsci 14,

43126 Parma,

Italy.

Tel: +39 (0)521 033093; Fax: +39 (0)521 033076; E-mail address: matteo.goldoni@unipr.it

Key words**:** Cobalt oxide nanoparticles; titanium oxide nanoparticles; endothelial cells; oxidative stress; inflammation.

ABSTRACT

Ultra-fine particles have recently been included among the risk factors for the development of endothelium inflammation and atherosclerosis, and cobalt (CoNPs) and titanium oxide nanoparticles (TiNPs) have attracted attention because of their wide range of applications. We investigated their toxicity profiles in two primary endothelial cell lines derived from human aorta (HAECs) and human umbilical vein (HUVECs) by comparing cell viability, oxidative stress, the expression of adhesion molecules and the release of chemokines during NP exposure. Both NPs were very rapidly internalised, and significantly increased adhesion molecule (ICAM-1, VCAM-1, E-selectin) mRNA and protein levels and the release of monocyte chemoattractant protein-1 (MCP-1) and interleukin 8 (IL-8). However, unlike the TiNPs, the CoNPs also induced time- and concentration-dependent metabolic impairment and oxidative stress without any evident signs of cell death or the induction of apoptosis. There were differences between the HAECs and HUVECs in terms of the extent of oxidative stress-related enzyme and vascular adhesion molecule expression, ROS production, and pro-inflammatory cytokine release despite the similar rate of NP internalisation, thus indicating endothelium heterogeneity in response to exogenous stimuli. Our data indicate that NPs can induce endothelial inflammatory responses via various pathways not involving oxidative stress.

INTRODUCTION

Nanotechnologies based on the chemical, mechanical, optical, magnetic and biological properties of nanomaterials are being increasingly used in a wide range of industries, and there are now more than 1,500 commercial products available on the world market (EPA, 2007). However, their use (which is still largely unregulated) has become a recognised social health problem because the inhalation, dermal absorption or ingestion of particles of various sizes and compositions leads to increased rates of chronic respiratory and cardiovascular diseases (Borm et al., 2004; Byrne and Baugh, 2008; Donaldson et al., 2013; Donaldson and Seaton, 2012; Oberdorster et al., 2005; Xia et al., 2009). It is currently difficult to quantify the risk because the available information is contradictory, and there is a lack of definite toxicological data or shared guidelines (Borm et al., 2006; Iavicoli et al., 2009; Schulte and Salamanca-Buentello, 2007), but there is clearly an urgent need to develop a rapid, accurate and efficient means of assessing the effects of nanoparticles (NPs) on human health.

Despite their limitations, *in vitro* studies are still fundamental when assessing dosing ranges and probable mechanisms of toxicity. In the case of metal or metal oxide NPs, besides modifications of cellular functions, such as repression/activation of genes and mitochondrial dysfunction (Comfort et al., 2014; Jeng and Swanson, 2006; Jugan et al., 2012; Karlsson et al., 2008; Soto et al., 2007), oxidative stress is one of the most studied mechanism of cytotoxicity. It occurs at early stages of interaction and is relevant to potential negative effects on cell functions and DNA damage (Carlson et al., 2008; Choi et al., 2009; Jugan et al., 2012; Karlsson et al., 2008; Liu et al., 2010; Moller et al., 2010; Papis et al., 2009).

Cobalt oxide (Co) is one of the most interesting NP chemicals because it can be used in pigments, catalysts, electrochemical sensors, and magnetism and energy storage. However, it has been reported that cobalt oxide NPs are associated with genotoxicity, an increased production of reactive oxygen species (ROS), and the induction of DNA fragmentation in humans (Alarifi et al., 2013; Colognato et al., 2008; De Boeck et al., 2003; Horev-Azaria et al., 2011; Papis et al., 2009).

The most widely synthesised and distributed of the metal oxide NPs are titanium dioxide (TiO_2) NPs. Micro- or submicro-particles have been commercially used as white pigments in paints, plastics, paper, pharmaceuticals, cosmetics and toothpastes. Furthermore, in addition to its industrial and medical applications, TiO_2 is also a common additive in many foods (Weir et al., 2012), and its use is exponentially increasing because of its stability, anti-corrosiveness and photocatalytic properties. It has been estimated that the global production of Ti nano-scaled particles was 5,000 t in 2010, and this is expected to increase further because of the greater use of personal care products such as topical sunscreens and cosmetics (EPA, 2009; Hendren et al., 2011; Robichaud et al., 2009). Consequently, there are many potential environmental and occupational sources of exposure to nanoscale TiO_2, but no definite toxicological profile has yet been published. The National Institute for Occupational Safety and Health (NIOSH) considers that occupational exposure (mainly via inhalation and dermal contact) to low concentrations of TiO_2 lead to a negligible risk of lung cancer in workers. Therefore, time-weighted average (TWA) airborne concentration limits of 2.4 mg/m^3 for fine and 0.3 mg/m^3 for ultra-fine TiO_2 for up to 10 hours/day during a 40-hour working week is recommended (NIOSH, 2011).

The inhaled, dermal or gastrointestinal intake of NPs can reach the bloodstream and be distributed to target organs distant from the site of adsorption (Christensen et al., 2011; Kreyling et al., 2002; Landsiedel et al., 2012; Nemmar et al., 2002). The endothelium lining the inner surface of blood vessels therefore comes into direct contact with NPs in a potentially pathogenic manner. Endothelial cells play a very important role in inflammation, and pro-inflammatory stimulation enhances the expression of adhesion molecules on cell membranes and thus mediates leukocyte attachment. Furthermore, these cells release potent cytokines, thus leading to the migration of leukocytes from blood into the perivascular space. The ability of metal NPs such as Co and Ti oxide to activate endothelial cells and induce pro-inflammatory events and the expression of early and late adhesion molecules has been demonstrated by *in vitro* studies (Duffin et al., 2007; Gojova et al., 2007; Han et

al., 2013; Iavicoli et al., 2012; Montiel-Davalos et al., 2012; Moschini et al., 2013; Peters et al., 2004; Strobel et al., 2014).

The aim of this *in vitro* study was to compare the anti-proliferative activity and cytotoxic effects of commercially available Co_3O_4 and TiO_2 nanopowders on human aortic endothelial cells (HAECs) and human umbilical vein endothelial cells (HUVECs) in an attempt to cast some light on their role and possible mechanisms of action in determining cell behaviour and fate. Previous studies of NPs have examined only one endothelial cell line, but studies of endothelial cell diversity have shown that ECs from different vascular beds have distinct sensitivities to oxidative stress and phenotypes that may contribute to the site specificity of vascular pathogenesis (Cai, 2005; Chi et al., 2003; Deng et al., 2006).

EXPERIMENTAL PROCEDURES

Reagents

The sterile plastic material for the tissue cultures was purchased from Costar, Corning (Amsterdam, The Netherlands), and phosphate buffered saline (PBS) from Euroclone (Milan, Italy). The ApoTox-Glo™ Triplex assay, the CytoTox-One™ homogeneous membrane integrity assay, and the CellTiter-Glo® luminescent cell viability assay were obtained from Promega (Madison, WI, USA), and the Annexin V/FITC kit from Bender MedSystems GmbH (Vienna, Austria). DCFH-DA was provided by Molecular Probes (Eugene, OR, USA), the JC-1 mitochondrial membrane potential assay kit by Biotium Inc. (Hayward, CA), the GSH colorimetric kit and GRP78 enzyme-linked immunosorbent assay (ELISA) by Enzo Life Sciences International Inc. (Plymouth Meeting, PA, USA), and the BCA protein assay by Thermo Scientific (Rockford, IL, USA). The MCP-1 ELISA kit was purchased from R&D Systems (Minneapolis, MN, USA) and the IL-8 US ELISA kit from Invitrogen (Camarillo, CA, USA). The FITC mouse anti-human CD106 (VCAM-1), PE mouse anti-human CD62E (E-selectin), and APC mouse anti-human CD54 (ICAM-1) antibodies and their respective isotype controls were purchased from Becton Dickinson (Lincoln Park, NJ, USA). The

commercially available cobalt (II,III) oxide (<50 nm) and TiO_2 (<100 nm) nanopowders were provided with physicochemical characterisation by Sigma (St. Louis, MO, USA), which also supplied all of the other reagents unless otherwise specified.

Particle preparation

The nano-sized Co(II,III) oxide and TiO_2 powders were suspended in ultra-pure water (2 mg/ml), sonicated on ice at 50 W using a probe sonicator (Heat Systems Ultrasonics Inc., Farmingdale, NY, USA) in order to minimise particle aggregates, stabilised by adding PBS 10x and bovine serum albumin (BSA) (final concentration 0.15%), and finally diluted in culture medium to the final working concentrations.

In order to distribute the particles in the working solution as evenly as possible before each cell culture experiment, the samples were processed three times by means of 20-second sonications immediately before use.

Characterisation of nanoparticles

The CoNPs and TiNPs were structurally and morphologically characterised by means of transmission electron microscopy (TEM) using a 200 kV analytical JEM 2200-FS (JEOL Inc., Peabody, MA, USA). As the behaviour and aggregation of the NPs in different media greatly depends on the surface charge of the NPs and the ionic strength of the suspension, the samples were further characterised using dynamic light scattering (DLS) and Z-potential techniques, and measurements made using a 90Plus PALS instrument (Brookhaven Instruments Corporation, Holtsville, NY, USA). In order to estimate the Stokes-Einstein or hydrodynamic radius (R_H) of the suspended NP agglomerates, we measured the autocorrelation function, which was fitted using the minimisation by non-negative least-squares (NNLS) technique, assuming the log-normal distribution of relaxation times in order to take into account the poly-dispersion of the not-ideal colloidal systems.

The specimens for TEM analysis were prepared by depositing one drop of a colloidal suspension of the nanoparticles in water (concentration: 0.1 mg/mL) on a TEM grid after 10 minutes of ultra-

sonication. More diluted colloidal suspensions (concentration: 0.01 mg/mL) were prepared for DLS and Z-potential characterisation by dispersing the NPs in different media and ultra-sonicating for 15 minutes.

Raman measurements were made using a Horiba Jobin-Yvon Labram micro-Raman apparatus (Longjumeau, France) equipped with an Olympus BH-4 confocal microscope with 4x, 10x, 50x, ULWD 50x and 100x objectives (lateral spatial resolutions of approximately 25, 10, 2, 2 and 1 µm). The spectrometer has a 20 mW He-Ne laser emitting at 632.8 nm, an edge filter, a 256 x 1024 pixel CCD detector, a 1800 grooves/mm grating, and a density filter wheel. Spectral resolution is about 1 cm^{-1}. The calibration of the spectrometer was controlled on the silicon Raman peak at 520.6 cm^{-1}. The spectra were recorded at 10 different points for each powder sample using the 4x and 10x objectives for 2-5 seconds and 5-8 repetitions. Baseline subtraction with a second-degree degree polynomial curve, normalisation and peak fitting were carried out using the Horiba Jobin-Yvon LABSPEC 5.78.24 software package.

A calibration curve designed to determine the amount of anatase in the TiNP powder was created by collecting the Raman spectra of x-ray diffraction (XRD) tested mixtures of anatase and rutile laboratory references at nine compositions ranging from 100 wt% anatase to 100 wt% rutile. The different ratios (R) of the areas (A) of selected anatase and rutile Raman bands ($R_{516/445}= A_{516} / (A_{516} + A_{445})$, $R_{143/445}= A_{143} / (A_{143} + A_{445})$, $R_{143/609}= A_{143} / (A_{143} + A_{609})$, and $R_{516/609}= A_{516} / (A_{516} + A_{609})$ were determined as a function of the anatase content *x* (wt%) using a peak-fitting procedure,.

The function $y=ax/(ax+100-x)$ was used to fit the data, where *a* is a fitting parameter taken as the ratio of the Raman absolute intensities of selected anatase and rutile bands. The fitting curves with a goodness of fit parameter (R^2) of ~0.99 (not shown) were used to determine the *x* value of the TiNPs in the commercial product.

Cell culture and treatment

The HAECs and HUVECs (purchased from Lonza, Basel, Switzerland) were grown in a fully supplemented EGM-2MV Bullet Kit (Lonza, Basel, Switzerland) and maintained at 37° in a 5% CO_2 humidified incubator, and used at passages 3-7 in the experiments. Before the treatments, 1 $\times 10^4$ cells/cm^2 were seeded in plates or flasks and cultured to 80-90% confluence, and were then incubated with NP concentrations ranging from 1 to 100 μg/mL for different time intervals. The control cells were incubated in particle-free medium.

Cell proliferation/viability studies

The cells were plated in clear-bottomed, white 96-well plates (100 μL per well) and, when they were 80% confluent, increasing concentrations of NPs were added to the medium and the cells left exposed for 24 or 48 hours. Three experiments were carried out for each exposure time.

The morphology of the cells and NP uptake were monitored using an inverted microscope (Olympus CK40-RFL, Tokyo, Japan). The proportions of viable and damaged cells were determined using the ApoTox-Glo™ Triplex and CytoTox-One™ homogeneous membrane integrity assays following the manufacturer's instructions. The CytoTox-One™ assay was not only used to evaluate the spontaneous release of lactate dehydrogenase (LDH) into the surrounding culture medium from cells with damaged membranes, but also to estimate the total number of cells in the assay wells at the end of the treatments. This procedure involved the lysis of all the cells in order to release LDH, and the total number of cells is directly proportional to the fluorescence representing LDH activity. Intracellular levels of ATP were quantified using the CellTiter-Glo luminescent cell viability assay, according to the manufacturer's recommendations.

Luminescence/fluorescence was detected using a Cary Eclipse fluorescence spectrophotometer (Varian, Inc., Palo Alto, CA, USA) and relative cell viability normalised against control values was used in the analysis.

Cell cycle

Cell phase distribution was assayed by determining the DNA content of the nuclei by means of flow cytometry. Briefly, after treatment with the NPs, the cells were collected, washed in PBS, and fixed in ethanol (96%). They were then stained by propidium iodide-PI (20 µg/mL in PBS containing RNase-A) at 4°C overnight. The analysis was made using a FC500™ flow cytometer (Beckman Coulter, Brea, CA, USA), and cell cycle phase distribution was calculated as percentages using FlowJo software (Ashland, OR, USA).

Uptake

A the FC500™ flow cytometer (Beckman Coulter, Brea, CA, USA) was used in this study. We determined uptake of NPs in three independent experiments, as described previously by Zucker *et al*. (2010). The highest dose of nanoparticles was run first to optimize dynamic ranges.

Apoptosis analysis

The supernatants of the cultures exposed to NPs for 24 hours, and the attached cells were harvested by means of trypsinisation and mixed with the corresponding supernatants before being washed with PBS. After incubation with FITC-labelled Annexin V and propidium iodide (PI) at room temperature for 15 minutes in the dark, the HAECs and HUVECs were analysed using a FC500™ flow cytometer (Beckman Coulter, Brea, CA, USA). Twenty thousand cells were counted for each measurement, and the dot plots and histograms were analysed using FlowJo software (Ashland, OR, USA). The annexin V-positive and PI-negative cells were considered to be in an early apoptotic phase; the cells positive for both annexin V and PI were considered to be in a late apoptotic/necrotic phase; and the cells negative for both annexin V and PI were considered viable.

Caspase 3 activity was evaluated using the ApoTox-Glo™ triplex assay in accordance with the manufacturer's protocol. The cells were cultured and treated with NPs in 96-well, clear-bottomed white plates, and luminescence was measured by means of a Cary Eclipse fluorescence spectrophotometer (Varian, Inc., Palo Alto, CA, USA).

Mitochondrial transmenbrane potential

The changes in mitochondrial membrane potential were monitored by 5,5′ ,6,6′ -tetrachloro-1,1′ ,3,3′ -tetraethyl-benzimidazolcarbocyanineiodide (JC-1), a lipophilic slow membrane redistribution dye. The green monomeric form of this dye in the cytosol and the red concentrated aggregates in the mitochondria were analyzed either by flow cytometer or by fluorescence plate reader, according to the manufacturer's protocols.

After treatment with NPs, the cells were detached by trypsin, washed in PBS, and incubated for 15 minutes in reagent solution at 37 C, 5% CO2. Mitochondria containing red JC-1 aggregates were detected in FL2 channel, and green JC-1 monomers were detected in FL1 channel of a FC500 flow cytometer (Beckman Coulter, Brea, CA, USA).

Staining of monolayer cells was carried out in 96-well plates and a Cary Eclipse fluorescence spectrophotometer (Varian, Inc., Palo Alto, CA, USA) was used to measure red fluorescence (excitation 550 nm, emission 600 nm) and green fluorescence (excitation 485 nm, emission 535 nm). The red/green ratio was calculated for each condition.

GRP78 enzyme-linked immunosorbent assay

Glucose-regulated protein (GRP78), also known as binding immunoglobulin protein or BiP, was quantified in cell lysates using a commercially available competitive enzyme-linked immunosorbent assay (ELISA) in accordance with the manufacturer's instructions. The values were normalised to protein concentrations and expressed as percentages of the controls.

Oxidative stress

The formation of intracellular reactive oxygen species (ROS) was revealed using 2,7-dichlorodihydrofluorescein diacetate (DCFH-DA), a non-polar and non-fluorescent compound that diffuses into the cytoplasm where intracellular esterases cleave the acetate group to yield polar, non-fluorescent 2′,7′-dichlorofluorescein (DCF), whereas its reaction with ROS forms a highly fluorescent two-electron oxidation product. The HAECs and HUVECs were pre-treated with 10 μM DCFH-DA in PBS at 37°C for 30 minutes in the dark, and then incubated with NPs before being

harvested, washed with PBS, and analysed by means of an FC500™ flow cytometer (Beckman Coulter, Brea, CA). Hydrogen peroxide (10 µM) was used as a positive control.

Lipid peroxidation was evaluated using the thiobarbituric acid reactive substances (TBARS) method as previously described (Bisceglie et al., 2013): the condensation of malondialdehyde (MDA) derived from polyunsaturated fatty acids with two equivalents of thiobarbituric acid gives a fluorescent red derivative that can be quantified using a Cary Eclipse fluorescence spectrophotometer (Varian, Inc., Palo Alto, CA) (excitation 515 nm, emission 545 nm).

Intracellular levels of glutathione (GSH and GSSG) were determined using a commercial colorimetric assay (Enzo Life Sciences International Inc., Plymouth Meeting, PA) in fresh cell lysates prepared in accordance with the manufacturer's protocol. The absorbance of the chromophoric thione produced was read at 405 nm in a Multiskan Ascent microwell plate reader (Thermo Labsystems, Helsinki, Finland).

The values of these three parameters were normalised to protein concentrations and expressed as percentages of the controls.

MCP-1 and IL-8 release

Immediately after nanoparticle incubation, the cell culture supernatants were collected and centrifuged at 16,000 × *g* for 5 minutes to remove cell debris and particles. The concentrations of interleukin 8 (IL-8 or CXCL-8) and monocyte chemoattractant protein-1 (MCP-1) were measured using commercially available ELISAs following the manufacturer's instructions, and were normalised to the number of cells. The chemokine concentrations in the medium of the treated cells were compared to the concentrations in the medium of untreated cells at each time point.

Cell surface expression of ICAM-1, VCAM-1 and E-selectin

The cell surface expression of intercellular adhesion molecule 1 (ICAM-1), vascular cell adhesion molecule 1 (VCAM-1) and E-selectin was assessed using specific fluorochrome-labelled monoclonal antibodies: FITC mouse anti-human CD106 for VCAM-1, PE mouse anti-human CD62E for E-selectin, and APC mouse anti-human CD54 for ICAM-1. The detached cells were

washed with ice-cold PBS without Ca^{++} and Mg^{++}, and incubated with the fluorescent antibodies for 30 minutes in the dark before flow cytometry analysis (FC500™ flow cytometer, Beckman Coulter, Brea, CA, USA). Isotype controls were included.

Protein determination

Protein concentrations were measured using a bicinchoninic acid (BCA) protein assay in accordance with the manufacturer's microwell plate protocol: bovine serum albumin dilutions were included as standard curves. Absorbances were read at 550 nm in a Multiskan Ascent microwell plate reader (Thermo Labsystems, Helsinki, Finland).

RNA isolation and gene expression

Total RNA was extracted from 10^5 cells using commercially available TRIzol (Ambion, Life Technologies, CA) and digested with DNase I (DNA-free kit, Ambion, Life Technologies, CA) in order to remove any genomic DNA contamination. After assessing the purity of the extract and quantifying the RNA (agarose gel electrophoresis and fluorimetric measurements), cDNA was synthesised using a commercial kit based on the use of inverse transcriptase , and amplified by means of real-time PCR (RT-PCR) using specific primers including exon-exon junctions specifically designed for heme-oxygenase 1 (HO-1), superoxide dismutase 1 (SOD-1), superoxide dismutase 2 (SOD-2), E-selectin (SELE), ICAM-1 and VCAM-1. After normalisation with phosphoglycerate kinase 1 (PGK1), hypoxanthine-guanine phosphoribosyltransferase (HPRT) and ribosomal protein L13 (RPL13) as housekeeping genes, the relative quantitative expression of the transcripts was calculated using geNorm software for Microsoft Excel™ (Vandesompele *et al.*, 2002).

Statistical analysis

The experimental results are expressed as mean values ± SD. All of the experiments were performed in triplicate and replicated at least three times. The experimental groups were compared using SPSS 17.0 software (SPSS Inc., Chicago, IL) and one-way ANOVA with Dunnett's or Turkey's *post hoc* tests; p values of ≤ 0.05 were considered statistically significant.

RESULTS

Nanoparticle characterisation

Transmission electron microscopy of the CoNPs showed that they had an irregular non-spherical shape, and tended to form agglomerates of tens of NPs (Fig. 1A); their narrow size distribution (std = 0.36) was centred around a mean value of 17 nm (Fig. 1C). The TiNPs had a regular spherical shape and were slightly aggregated (Fig. 1B); they had a wide size distribution (std = 0.57) centred around a value of 38 nm (Fig. 1D).

The estimated specific surface areas of the Co_3O_4 and TiO_2 NPs were respectively 46.7 m^2/g and 13.8 m^2/g.

The behaviour of CoNPs and TiNPs suspended in different media was compared using DLS measurements. Figures 1E and 1F respectively show the size distributions CoNPs and TiNPs obtained by fitting the experimental data. In water, CoNPs had a greater tendency to form clusters than TiNPs (the blue lines in Figs. 1E and 1F) whereas, in cell culture media, TiNPs had a greater tendency to cluster than in an aqueous solution (the size distribution peak shifted to higher values of R_H) and the size distribution of the clusters of CoNPs broadened. These behaviours clearly agreed with the measured Z-potential values shown in Table 1. TiNPs tended to agglomerate less than CoNPs in water because of the more efficient stabilisation provided by their higher surface charge. As expected, the surface charge of the NPs was reduced in the investigated cell culture media, probably probably because their coverage by a protein corona led to some changes in cluster size.

The Raman spectra of the TiNPs (not shown) had peaks corresponding to a mixture of anatase (a tetragonal polymorph, space group $I4_1/amd$, characterised by Raman peaks at ~143, 196, 396, 516 and 638 cm^{-1}) and rutile (a tetragonal polymorph, $P4_2/mnm$, with characteristic Raman peaks at ~143, 238, 445 and 609 cm^{-1}) (Djaoued et al., 2002). All of the TiNP peaks were broader than those of pure polymorphs, thus confirming the presence of nanosized (<100 nm) TiO_2 particles (Bersani et al., 1998). In line with these findings, the results of the procedure described in Experimental Procedures indicate 93 wt% anatase in the TiO_2 powder with an estimated uncertainty of ± 1%.

Cell uptake

The optical microscope observations suggest that the NPs and aggregates of both metal oxides gradually sedimented onto endothelial cells, passed through the cell membrane, and then accumulated within the cytoplasm surrounding the nucleus: low NP concentrations led to individual visible aggregates, whereas the cells treated with high concentrations had coarse aggregates throughout the cytoplasm. In all cases, the NPs tended to form a perinuclear ring and the nucleus was outlined by NPs.

NP uptake led to dose- and time-dependent changes in physical parameters, with TiNPs being the most effective. The cytogram distribution showed increased side scatter (SSC) intensity (Fig. 2A), and these changes in SSC distribution were clearly evident 30 minutes after the beginning of exposure to TiNPs. Figure 2B shows the mean SSC ratios of NP-treated HAECs and HUVECs over 24 hours: in both cases, NP uptake was very rapid in the first half-hour, but a plateau was reached in the cells treated with CoNPs after one hour, and in the cells treated with TiNPs after six hours.

The increase in SSC was accompanied by a non-significant, concentration-dependent decrease in forward scatter (FSC), but this parameter was less sensitive than SSC and was probably influenced by the SSC signal: light scattered in all directions and was not transmitted to the FSC detector.

Cell viability and proliferation

The effects of the NPs on cell viability and proliferation were assessed using three different assays, the results of which were confirmed by microscopic observations and cell counting.

HAECs and HUVECs showed slightly different patterns of response to decreasing NP concentrations (range 100-1 µg/mL) (Fig. 3). The CoNPs and TiNPs did not cause any changes in the number of HAECs (evaluated by measuring complete LDH) or induce necrosis as evaluated by measuring spontaneous LDH release. The antiproliferative effects of the highest CoNP concentration (100 µg/mL) on HUVECs were first observed after 24 hours, whereas 100 µg/mL of TiNPs significantly inhibited HUVEC proliferation (-32%) only after 72 hours (data not shown).

Furthermore, 24 and 48 hours of exposure to CoNPs (but not TiNPs) significantly inhibited protease activity and decreased intracellular ATP concentrations in both cell lines, with the greatest effect being observed after 48 hours' exposure to a concentration of 100 µg/mL, thus indicating the time- and dose-dependent impairment of metabolically active cells.

These findings are consistent with the analysis of cell cycle progression (Fig. 4), which was significantly perturbed in both cell lines: the number of HAECs and HUVECs accumulated in phase G0/G1 after 24 hours of treatment.

In order to determine whether these effects were associated with apoptosis, caspase-3 activation and phosphatidylserine translocation were evaluated after 24 hours' exposure, but no significant differences were observed (data not shown).

No significant differences were observed as compared to controls looking at mitochondrial transmenbrane potential (NPs 20 µg/ml, 4 and 24 h of exposure, data not shown) and GRP78/BIP levels (NPs 20 µg/ml, 8 and 24 h of exposure, data not shown).

Oxidative stress

Intracellular ROS were assayed early (after 30 and 60 minutes) because of their instability (Fig. 5A). In comparison with controls, CoNPs induced intracellular ROS in a dose- and time-dependent manner: after 60 minutes, the highest CoNP concentration (50 µg/mL) led to a 47.2% increase in HAECs and a 78.8% increase in HUVECs. ROS production was associated with lipid peroxidation (TBARS test, Fig. 5B) and GSH scavenger activity (Fig. 5C): CoNPs 20 µg/mL caused an early, time-limited decrease in GSH levels in HUVECs, and a significant increase (40.8%) of its oxidised form (GSSG) in HAECs after four hours (data not shown). TiNPs did not induce ROS production or elicit lipid peroxidation or glutathione consumption at any concentration or time.

Antioxidant enzyme gene expression

In order to determine the effect of CoNPs and TiNPs on antioxidant enzyme gene expression, HAECs and HUVECs were incubated with NPs 20 µg/mL (a concentration that did not affect their proliferation and viability) for different periods of time, and the results were compared with those

observed in cells grown in particle-free medium. CoNPs induced HO-1 expression in both cell lines, but with some differences (Fig. 5D): it gradually and significantly increased in HAECs between the fourth and twelfth hour of exposure ($P<0.001$), and then significantly decreased until the 24th hour, thus indicating cell recovery, but significantly increased throughout the 24 hours in HUVECs ($P<0.001$). Furthermore, HO-1 expression was approximately five times higher than in HAECs. There was no SOD-1 or SOD-2 gene expression at any of the considered times (data not shown).

TiNPs did not induce any antioxidant enzyme gene expression at any of the studied doses or time points.

MCP-1 and IL-8 protein release

Both NPs induced the release of MCP-1 and IL-8 by the cultured HAECs and HUVECs, with TiNPs being the most effective (Fig. 6).

Adhesion molecule gene expression

To determine the effect of Co NPs and TiNPs on SELE, VCAM-1 and ICAM-1 gene expression, HAEC and HUVEC cells were incubated with the NPs at a concentration of 20 μg/mL for different times; the controls were cells grown in particle-free medium. In the HAECs treated with CoNPs, SELE gene expression increased after four hours ($p<0.01$) and then gradually decreased to control levels after 24 hours; peak VCAM-1 and ICAM-1 gene expression was observed after eight hours' treatment. TiNP treatment increased SELE expression about 15 times after eight hours, and the levels returned to those of the control after 24 hours; trend of VCAM-1 and ICAM-1 gene expression was the same trend but quantitatively less (Tab. 2).

CoNP treatment of HUVECs, increased ICAM-1 ($p<0.001$) and VCAM-1 expression ($p<0.01$) after four hours, both of which returned to control level after 12 hours; SELE expression was not significant. TiNPs induced VCAM-1 and SELE expression in a time-dependent manner, with a peak after four hours; ICAM-1 was not significantly expressed. These findings were confirmed by flow cytometry.

DISCUSSION

This study compared the effects of two different metal oxide NPs on two endothelial cell lines derived from different vascular beds but, before analysing the NP-induced cell responses, it is important to comment on the reliability of the toxicity assays because it has been reported that dyes and probes can interact with or absorb NPs and lead to invalid results (Darolles et al., 2013; Han et al., 2011; Love et al., 2012; Monteiro-Riviere et al., 2009). The results of our LDH, ATP and protease assays were consistent with the microscopy findings, and our DCFH-DA measurements of intracellular ROS production were confirmed by specific markers of oxidative lipid damage and enzyme expression. However, the MTT assay proved to be unsuitable for assessing the cytotoxicity of CoNPs because the strong reaction and colour development indicated interference with the metal oxide. Our observations underline the fact that the choice of dyes, probes and tests is critical for *in vitro* studies investigating the interactions of metallic NPs with biological systems, the suitability of which should be evaluated case by case. For all of these reasons, we combined various cytotoxicity assays (Han et al., 2011).

We studied Ti and Co oxide nanoparticles as examples of metal oxides involved with environmental and occupational exposure, and used the differences in toxicity (Peters et al., 2004) induced by their different compositions, sizes and solubility to elucidate the underlying toxic mechanisms. Nano-sized Co oxide is one of the most biologically reactive metal oxides and this raises concerns about the safety of using it for production purposes and, although Ti used to be considered a harmless non-toxic metal and was frequently used as a negative control when assessing nanotoxicity, the increasing use of these particles in consumer products and the growing understanding of their properties have raised questions concerning their toxicological potential (Skocaj et al., 2011). In many *in vitro* and *in vivo* systems adverse effects have been reported with higher toxicity of size-decreasing NPs and of the anatase crystal form (Bhattacharya et al., 2009; Chen et al., 2014; Han et al., 2013; Iavicoli et al., 2011; Johnston et al., 2009; Kenzaoui et al., 2012; Landsiedel et al., 2010; Liu et al., 2010; Montiel-Davalos et al., 2012; Petkovic et al., 2011). Other studies excluded TiNPs

cytotoxic effects also in acute exposure conditions (Moschini et al., 2013; Peters et al., 2004; Prasad et al., 2014; Pujalte et al., 2011; Strobel et al., 2014). The data published so far are not suitable for risk assessment and management (Iavicoli et al., 2011; Valant et al., 2012).

The discrepancies in the findings of studies of TiNPs (and, more generally, other NPs) may not only be due to differences in the nature and size of the particles, but also to the different protocols used for preliminary NP dispersion (e.g. in water or media containing PBS, BSA, or fetal calf serum) as different methods may influence the properties of NP preparations, such as their size or surface coat (Bihari et al., 2008). This poses a considerable problem for standardising studies of NPs because their biological effect seems to depend on their protein "corona", the biomolecules adsorbed on their surface (Lundqvist et al., 2008; Lynch et al., 2007; Monopoli et al., 2013). It has been suggested that the presence of serum or BSA in culture media leads to different nano-TiO_2 agglomerate profiles, and that the smaller particles are associated with increased cellular interactions and effects (Prasad et al., 2013). In order to mimic the endothelial environment, we used serum albumin (the main blood protein) in the NP preparations, and so it was expected that albumin may be selectively adsorbed before cell uptake. The presence of 2% foetal bovine serum in the culture medium can complete the protein corona of the studied nanoparticles, but we did not observe any differences in the viability and oxidative stress of HAECs and HUVECs treated with NPs diluted in PBS without BSA (data not shown).

Microscopy has shown that TiNPs and CoNPs entering human endothelial cells create rings around the nuclei, but the extent of their intracellular uptake depends on the characteristics of the NPs. Our data confirm that NP uptake can easily be monitored by means of flow cytometry (Zucker et al., 2010). SSC intensity is mainly related to the internal structure and the number and type of organelles present in a cell, and so it is used to reveal differences in the physical state of a cell and to define cell populations.

Our findings clearly demonstrate that even very high concentrations of TiO_2 nanoparticles have few acute cytotoxic effects on HAECs and HUVECs, whereas CoNPs impair cell metabolism in a concentration- and time-dependent manner.

However, they also suggest that cells are affected by the presence of NPs even in the absence of evident cellular death and mitochondrial dysfunction. Although both cell types showed a low toxic response to NPs (as assessed on the basis of cell growth and cell membrane integrity), we recorded significant alterations and the activation of gene stress markers indicating the triggering of stress-related signalling pathways before the onset of the "classical" signs of cytotoxicity. TiNP treatment of human endothelial cells was associated with a number significant biochemical changes. The absence of an effect on cell viability may reflect the relatively brief time of exposure (24 hours) as metabolic effects may precede effects on cell viability (Tucci et al., 2013).

Although other authors have reported significant effects (Montiel-Davalos et al., 2012), our results are in line with those of Strobel *et al.* (2014), who found that TiNPs had only slight effects on endothelial cells that were only detectable at concentrations of 100 µg/ml. Nevertheless, they also suggested that the low cellular ATP levels observed after 24 hours may be related to the energy-consuming mechanism of uptake of TiNPs (Strobel et al., 2014), whereas we observed a decrease in ATP levels in both cell lines during treatment with CoNPs, but not during treatment with TiNPs. HAECs and HUVECs actively incorporated both NPs, but the uptake of TiNPs was very rapid (15 minutes), effective, and peaked within one hour.

One obvious candidate pathway for nanoparticle-induced endothelial inflammation and atherogenesis is the production of ROS, which has previously been shown to be common after treatment with NPs. Like previous authors (Alarifi et al., 2013; Colognato et al., 2008; Papis et al., 2009), we found that CoNPs rapidly induced ROS, but this was not an effect of TiNPs.

The events initiating inflammation include endothelial activation and monocyte/macrophage recruitment followed by their diffusion in subintimal space as a result of complex mechanisms. E-selectin facilitates the rolling of molecules on the surface of endothelium cells, after which adhesion

molecules such as VCAM-1 and ICAM-1 mediate the adhesion of blood leukocytes attracted by the chemokines in the activated area. Dysregulated adhesion molecule and cytokine expression has been found in atherosclerotic lesions, and is thought to play a very important role in the initial steps of atherosclerosis and its progression (Businaro et al., 2012). Our findings show that the direct and acute exposure of endothelial cells to NPs (including TiNPs) significantly increases the expression of SELE, ICAM-1 and VCAM-1, and the release of MCP-1 and IL-8 by endothelial cells even in the absence of significant oxidative stress (a response that can lead to leukocyte recruitment to an inflammatory site in the vascular endothelium). TiNPs contribute more than CoNPs to disturbing endothelium homeostasis and promoting endothelial dysfunction, thus laying the foundations for the further advancement of atherosclerosis. It is simple to attribute the endothelial activation induced by CoNPs to oxidative stress, but more difficult to explain this effect during TiNP exposure, although other responsive pathways such as endoplasmic reticulum (ER) stress might be involved (Chen et al., 2014; Christen et al., 2013; Tsai et al., 2011; Zhang et al., 2012). For this reason, we evaluated glucose-regulated protein (GRP78), a molecular chaperone located in the lumen of the ER that is involved in the folding and assembly of proteins, the transport of newly synthesised polypeptides across the ER membrane and the retrograde transport of aberrant proteins destined for degradation. Its synthesis is induced under conditions that lead to the accumulation of unfolded polypeptides in the ER and, given its function, it plays a fundamental initial role in ER stress. Although a specific and complete study involving ER stress should be performed (Chen et al., 2014), our preliminary result suggests that ER may be not the main target of NP toxicity.

TiO_2 nanoparticles can be considered relatively harmless to humans because *in vivo* endothelial cells would come into contact with very small amounts (Strobel et al., 2014). Nevertheless, the fast and efficient uptake of NPs into cells may lead to accumulation and subsequent endothelial injury after long-term exposure, possibly due to a Trojan-horse mechanism (Ortega et al., 2014). This is particularly relevant in the case of TiO_2 because typical exposure in an adult may be of the order of 1 mg of Ti per kilogram of body weight per day, mainly in nano-sized form (Weir et al., 2012).

Particular attention should therefore be paid to potential chronic effects because this material is massively taken up and retained in endothelial cells.

Any consideration of endothelial responses or injury to the vascular endothelium must taken into account the heterogeneity of the tissue. The vascular bed of origin greatly affects endothelial cell phenotype, constitutive gene and micro-RNA profile, protein expression and responsiveness (Aird, 2007; Chi et al., 2003; McCall et al., 2011; Nguyen et al., 2010; Wang et al., 2011), and molecular differences in cell-cell junctions, flow orientation, fenestration size and vesicle formation may explain why aortic and microvascular endothelial cells behave differently. Furthermore, anti-oxidative genes are more highly expressed in cultured vein than coronary artery cells (Deng et al., 2006), and HUVECs are particularly sensitive to oxidative damage (Cai, 2005).

The reason for the difference in metabolizing enzyme and cell adhesion molecule expressions between HAEC and HUVEC is not clear, as it has not been clarified by the numerous studies carried out (Szasz et al., 2007). These intrinsic profiles of ECs from different parts of vasculature ultimately may reflect the different gene expression patterns of arteries and veins, which persist for generation *in vitro*. ECs discriminate stimuli and the resulting phenotypes are specific to EC type and may be explained at least by the differing regulation of gene transcription level. These observations reveal the complexity of processes that regulates vasculature specific endothelial behavior and a need for the understanding of mechanisms for the differences in induced functional changes across the vascular bed.

Because of these phenotypic, genetic, and protein differences between endothelial cells from different vascular locations, we hypothesised that the response of HAECs and HUVECs to NPs may also vary, and our findings show that there are differences between the two in terms of oxidative stress-related enzyme and vascular adhesion molecule expression. HUVECs were more susceptible to the oxidative stress caused by CoNPs as assessed by the inhibition of proliferation and HO-1 expression, whereas VCAM-1 and E-selectin were more strongly expressed in HAECs in response to TiNPs. These results indicate that the heterogeneity of endothelial cells is not confined to

constitutive expression, but also affects the response to exogenous stimuli, and are supported by recent findings concerning differences between artery and vein biology under both physiological and pathophysiological conditions (Szasz et al., 2007).

Taken together, our data suggest that the intracellular presence of even apparently safe NPs can promote inflammatory processes that are probably mediated by multiple signalling pathways, and not only oxidative stress.

Acknowledgements

This study was supported by the Italian Ministry of Health Ricerca Finalizzata 2009 grant: Integrated approach to evaluating the biological effects on lung, cardiovascular system and skin of occupational exposure to nanomaterials (NanO I-LuCaS). RF-2009-1472550. The authors declare that they have no conflict of interest.

ABBREVIATIONS

BCA, bicinchoninic acid; CoNPs, nanoparticles of cobalt oxide; DCFH-DA, 2,7-dichlorodihydrofluorescein diacetate; EC, endothelial cells; FSC, forward scatter; GSH, glutathione; GSSG, glutathione disulfide; HAECs, human aortic endothelial cells; HO-1, heme oxygenase-1; HUVECs, human umbilical vein endothelial cells; ICAM-1, intercellular adhesion molecule 1; IL-8 (CXCL-8), interleukin 8; LDH, lactate dehydrogenase; MCP-1, monocyte chemoattractant protein-1; MDA, malondialdehyde; NPs, nanoparticles; SELE, E-selectin; ROS, reactive oxygen species; SSC, side scatter; SOD-1, superoxide dismutase 1; SOD-2, superoxide dismutase; TBARS, thiobarbituric acid reactive substances; TEM, transmission electron microscopy; TiNPs, nanoparticles of titanium dioxide; VCAM-1, vascular cell adhesion molecule 1.

REFERENCES

Aird, W.C., 2007. Phenotypic heterogeneity of the endothelium II. Representative vascular beds. Circul. Res. 100, 174-190.

Alarifi, S., Ali, D., Suliman Y, A.O., et al., 2013. Oxidative stress contributes to cobalt oxide nanoparticles-induced cytotoxicity and DNA damage in human hepatocarcinoma cells. Int. J. Nanomed. 8, 189-199.

Bersani, D., Lottici, P.P., Ding, X.Z., 1998. Phonon confinement effects in the Raman scattering by TiO2 nanocrystals. Appl. Phys. Lett. 72, 73-75.

Bhattacharya, K., Davoren, M., Boertz, J., et al., 2009. Titanium dioxide nanoparticles induce oxidative stress and DNA-adduct formation but not DNA-breakage in human lung cells. Part. Fibre Toxicol. 6, 17.

Bihari, P., Vippola, M., Schultes, S., et al., 2008. Optimized dispersion of nanoparticles for biological in vitro and in vivo studies. Part. Fibre Toxicol. 5, 14.

Bisceglie, F., Alinovi, R., Pinelli, S., et al., 2013. Ni(II) and Cu(II) N-4-ethylmorpholine citronellalthiosemicarbazonate: a comparative analysis of cytotoxic effects in malignant human cancer cell lines. Metallomics 5, 1510-1518.

Borm, P.J.A., Robbins, D., Haubold, S., et al., 2006. The potential risks of nanomaterials: a review carried out for ECETOC. Part. Fibre Toxicol. 3, 11.

Borm, P.J.A., Schins, R.P.F., Albrecht, C., 2004. Inhaled particles and lung cancer, part B: Paradigms and risk assessment. Int. J. Cancer 110, 3-14.

Businaro, R., Tagliani, A., Buttari, B., et al., 2012. Cellular and molecular players in the atherosclerotic plaque progression. Ann. N.Y. Acad. Sci. 1262, 134-141.

Byrne, J.D., Baugh, J.A., 2008. The significance of nanoparticles in particle-induced pulmonary fibrosis. McGill J. Med. 11, 43-50.

Cai, H., 2005. Hydrogen peroxide regulation of endothelial function: Origins, mechanisms, and consequences. Cardiovasc. Res. 68, 26-36.

Carlson, C., Hussain, S.M., Schrand, A.M., et al., 2008. Unique Cellular Interaction of Silver Nanoparticles: Size-Dependent Generation of Reactive Oxygen Species. J. Phys. Chem. B 112, 13608-13619.

Chen, R., Huo, L., Shi, X., et al., 2014. Endoplasmic reticulum stress induced by zinc oxide nanoparticles is an earlier biomarker for nanotoxicological evaluation. ACS Nano 8(3), 2562-2574.

Chen, Z., Wang, Y., Ba, T., et al., 2014. Genotoxic evaluation of titanium dioxide nanoparticles in vivo and in vitro. Toxicol. Lett. 226, 314-319.

Chi, J.T., Chang, H.Y., Haraldsen, G., et al., 2003. Endothelial cell diversity revealed by global expression profiling. Proc. Natl. Acad. Sci. U. S. A. 100, 10623-10628.

Choi, S.J., Oh, J.M., Choy, J.H., 2009. Toxicological effects of inorganic nanoparticles on human lung cancer A549 cells. J. Inorg. Biochem. 103, 463-471.

Christen, V., Capelle, M., Fent, K., 2013. Silver nanoparticles induce endoplasmatic reticulum stress response in zebrafish. Toxicol. Appl. Pharmacol. 272(2), 519-528.

Christensen, F.M., Johnston, H.J., Stone, V., et al., 2011. Nano-TiO2-feasibility and challenges for human health risk assessment based on open literature. Nanotoxicology 5, 110-124.

Colognato, R., Bonelli, A., Ponti, J., et al., 2008. Comparative genotoxicity of cobalt nanoparticles and ions on human peripheral leukocytes in vitro. Mutagenesis 23, 377-382.

Comfort, K.K., Braydich-Stolle, L.K., Maurer, E.I., et al., 2014. Less Is More: Long-Term in Vitro Exposure to Low Levels of Silver Nanoparticles Provides New Insights for Nanomaterial Evaluation. Acs Nano 8, 3260-3271.

Darolles, C., Sage, N., Armengaud, J., et al., 2013. In vitro assessment of cobalt oxide particle toxicity: Identifying and circumventing interference. Toxicol. In Vitro 27, 1699-1710.

De Boeck, M., Lombaert, N., De Backer, S., et al., 2003. In vitro genotoxic effects of different combinations of cobalt and metallic carbide particles. Mutagenesis 18, 177-186.

Deng, D.X., Tsalenko, A., Vailaya, A., et al., 2006. Differences in vascular bed disease susceptibility reflect differences in gene expression response to atherogenic stimuli. Circ. Res. 98, 200-208.

Djaoued, Y., Badilescu, S., Ashrit, P.V., et al., 2002. Study of Anatase to Rutile Phase Transition in Nanocrystalline Titania Films. J. Sol-Gel Sci. Technol. 24, 255-264.

Donaldson, K., Duffin, R., Langrish, J.P., et al., 2013. Nanoparticles and the cardiovascular system: a critical review. Nanomedicine 8, 403-423.

Donaldson, K., Seaton, A., 2012. A short history of the toxicology of inhaled particles. Part. Fibre Toxicol. 9, 13.

Duffin, R., Tran, L., Brown, D., et al., 2007. Proinflammogenic effects of low-toxicity and metal nanoparticles in vivo and in vitro: Highlighting the role of particle surface area and surface reactivity. Inhalation Toxicol. 19, 849-856.

EPA, U.S., 2007. EPA Nanotechnology White Paper U.S. Environmental Protection Agency, Washington, USA.

EPA, U.S., 2009. Office of Research and Development. Final Nanomaterial Research Strategy (NRS). U.S. Environmental Protection Agency, Washington, USA.

Gojova, A., Guo, B., Kota, R.S., et al., 2007. Induction of inflammation in vascular endothelial cells by metal oxide nanoparticles: Effect of particle composition. Environ. Health Perspect. 115, 403-409.

Han, S.G., Newsome, B., Hennig, B., 2013. Titanium dioxide nanoparticles increase inflammatory responses in vascular endothelial cells. Toxicology 306, 1-8.

Han, X., Gelein, R., Corson, N., et al., 2011. Validation of an LDH assay for assessing nanoparticle toxicity. Toxicology 287, 99-104.

Hendren, C.O., Mesnard, X., Droge, J., et al., 2011. Estimating Production Data for Five Engineered Nanomaterials As a Basis for Exposure Assessment. Environ. Sci. Technol. 45, 2562-2569.

Horev-Azaria, L., Kirkpatrick, C.J., Korenstein, R., et al., 2011. Predictive toxicology of cobalt nanoparticles and ions: comparative in vitro study of different cellular models using methods of knowledge discovery from data. Toxicol. Sci. 122, 489-501.

Iavicoli, I., Leso, V., Bergamaschi, A., 2012. Toxicological Effects of Titanium Dioxide Nanoparticles: A Review of In Vivo Studies. J. Nanomaterials 2012, 964381.

Iavicoli, I., Leso, V., Fontana, L., et al., 2011. Toxicological effects of titanium dioxide nanoparticles: a review of in vitro mammalian studies. Eur. Rev. Med. Pharmacol. Sci. 15, 481-508.

Iavicoli, S., Rondinone, B.M., Boccuni, F., 2009. Occupational safety and health's role in sustainable, responsible nanotechnology: gaps and needs. Hum. Exp. Toxicol. 28, 433-443.

Jeng, H.A., Swanson, J., 2006. Toxicity of metal oxide nanoparticles in mammalian cells. J. Environ. Sci. Health A-Tox. Hazard. Subst. Environ. Eng. 41, 2699-2711.

Johnston, H.J., Hutchison, G.R., Christensen, F.M., et al., 2009. Identification of the mechanisms that drive the toxicity of TiO2 particulates: the contribution of physicochemical characteristics. Part. Fibre Toxicol. 6, 33.

Jugan, M.L., Barillet, S., Simon-Deckers, A., et al., 2012. Titanium dioxide nanoparticles exhibit genotoxicity and impair DNA repair activity in A549 cells. Nanotoxicology 6, 501-513.

Karlsson, H.L., Cronholm, P., Gustafsson, J., et al. 2008. Copper oxide nanoparticles are highly toxic: A comparison between metal oxide nanoparticles and carbon nanotubes. Chem. Res. Toxicol. 21, 1726-1732.

Kenzaoui, B.H., Bernasconi, C.C., Guney-Ayra, S., et al., 2012. Induction of oxidative stress, lysosome activation and autophagy by nanoparticles in human brain-derived endothelial cells. Biochem. J. 441, 813-821.

Kreyling, W.G., Semmler, M., Erbe, F., et al., 2002. Translocation of ultrafine insoluble iridium particles from lung epithelium to extrapulmonary organs is size dependent but very low. J. Toxicol. Environ. Health A 65, 1513-1530.

Landsiedel, R., Fabian, E., Ma-Hock, L., et al., 2012. Toxico-/biokinetics of nanomaterials. Arch. Toxicol. 86, 1021-1060.

Landsiedel, R., Ma-Hock, L., Kroll, A., et al., 2010. Testing Metal-Oxide Nanomaterials for Human Safety. Adv. Mat. 22, 2601-2627.

Liu, S.C., Xu, L.J., Zhang, T., et al., 2010. Oxidative stress and apoptosis induced by nanosized titanium dioxide in PC12 cells. Toxicology 267, 172-177.

Love, S.A., Maurer-Jones, M.A., Thompson, J.W., et al., 2012. Assessing Nanoparticle Toxicity. Ann. Rev. Anal. Chem. 55, 181-205.

Lundqvist, M., Stigler, J., Elia, G., et al., 2008. Nanoparticle size and surface properties determine the protein corona with possible implications for biological impacts. Proc. Natl. Acad. Sci. U. S. A. 105, 14265-14270.

Lynch, I., Cedervall, T., Lundqvist, M., et al., 2007. The nanoparticle - protein complex as a biological entity; a complex fluids and surface science challenge for the 21st century. Adv. Colloid Interface Sci. 134-35, 167-174.

McCall, M.N., Kent, O.A., Yu, J.S., et al., 2011. MicroRNA profiling of diverse endothelial cell types. BMC Med. Genomics 4, 78.

Moller, P., Jacobsen, N.R., Folkmann, J.K., et al., 2010. Role of oxidative damage in toxicity of particulates. Free Radical Res. 44, 1-46.

Monopoli, M.P., Pitek, A.S., Lynch, I., et al., 2013. Formation and Characterization of the Nanoparticle-Protein Corona. Nanomaterial Interfaces in Biology: Methods and Protocols 1025, 137-155.

Monteiro-Riviere, N.A., Inman, A.O., Zhang, L.W., 2009. Limitations and relative utility of screening assays to assess engineered nanoparticle toxicity in a human cell line. Toxicol. Appl. Pharmacol. 234, 222-235.

Montiel-Davalos, A., Luis Ventura-Gallegos, J., Alfaro-Moreno, E., et al., 2012. TiO2 Nanoparticles Induce Dysfunction and Activation of Human Endothelial Cells. Chem. Res. Toxicol. 25, 920-930.

Moschini, E., Gualtieri, M., Colombo, M., et al., 2013. The modality of cell-particle interactions drives the toxicity of nanosized CuO and TiO2 in human alveolar epithelial cells. Toxicol. Lett. 222, 102-116.

Nemmar, A., Hoet, P.H.M., Thomeer, M., et al., 2002. Passage of inhaled particles into the blood circulation in humans - Response. Circulation 106, E141-E142.

Nguyen, V., Hanna, G., Rodrigues, N., et al., 2010. Differential proteomic analysis of lymphatic, venous, and arterial endothelial cells extracted from bovine mesenteric vessels. Proteomics 10, 1658-1672.

NIOSH, 2011. Current Intelligence Bulletin 63: Occupational Exposure to Titanium Dioxide. Department of Health and Human Services, Centers for Disease Control and Prevention, National Institute for Occupational Safety and Health, Atlanta, USA.

Oberdorster, G., Oberdorster, E., Oberdorster, J., 2005. Nanotoxicology: An emerging discipline evolving from studies of ultrafine particles. Environ. Health Perspect. 113, 823-839.

Ortega, R., Bresson, C., Darolles, C., et al., 2014. Low-solubility particles and a Trojan-horse type mechanism of toxicity: the case of cobalt oxide on human lung cells. Part. Fibre Toxicol. 11, 14.

Papis, E., Rossi, F., Raspanti, M., et al., 2009. Engineered cobalt oxide nanoparticles readily enter cells. Toxicol. Lett. 189, 253-259.

Peters, K., Unger, R.E., Kirkpatrick, C.J., et al., 2004. Effects of nano-scaled particles on endothelial cell function in vitro: Studies on viability, proliferation and inflammation. J. Mat. Sci.-Mat. Med. 15, 321-325.

Petkovic, J., Zegura, B., Stevanovic, M., et al., 2011. DNA damage and alterations in expression of DNA damage responsive genes induced by TiO2 nanoparticles in human hepatoma HepG2 cells. Nanotoxicology 5, 341-353.

Prasad, R.Y., Simmons, S.O., Killius, M.Get al., 2014. Cellular interactions and biological responses to titanium dioxide nanoparticles in HepG2 and BEAS-2B cells: role of cell culture media. Environ. Mol. Mutagen. 55, 336-342.

Prasad, R.Y., Wallace, K., Daniel, K.M., et al., 2013. Effect of Treatment Media on the Agglomeration of Titanium Dioxide Nanoparticles: Impact on Genotoxicity, Cellular Interaction, and Cell Cycle. Acs Nano 7, 1929-1942.

Pujalte, I., Passagne, I., Brouillaud, B., et al., 2011. Cytotoxicity and oxidative stress induced by different metallic nanoparticles on human kidney cells. Part. Fibre Toxicol. 8, 10.

Robichaud, C.O., Uyar, A.E., Darby, M.R., et al., 2009. Estimates of Upper Bounds and Trends in Nano-TiO2 Production As a Basis for Exposure Assessment. Environ. Sci. Technol. 43, 4227-4233.

Schulte, P.A., Salamanca-Buentello, F., 2007. Ethical and scientific issues of nanotechnology in the workplace. Environ. Health Perspect. 115, 5-12.

Skocaj, M., Filipic, M., Petkovic, J., et al., 2011. Titanium dioxide in our everyday life; is it safe? Radiol. Oncol. 45, 227-247.

Soto, K., Garza, K.M., Murr, L.E., 2007. Cytotoxic effects of aggregated nanomaterials. Acta Biomater. 3, 351-358.

Strobel, C., Torrano, A., Herrman, R., et al., 2014. Effects of the physicochemical properties of titanium dioxide nanoparticles, commonly used as sun protection agents, on microvascular endothelial cells. J. Nanoparticles Res.16, 2130.

Szasz, T., Thakali, K., Fink, G.D., et al., 2007. A comparison of arteries and veins in oxidative stress: Producers, destroyers, function, and disease. Exp. Biol. Med. 232, 27-37.

Tucci, P., Porta, G., Agostini, M., et al., 2013. Metabolic effects of TiO2 nanoparticles, a common component of sunscreens and cosmetics, on human keratinocytes. Cell Death Dis. 4, e549.

Tsai, Y.Y., Huang, Y.H., Chao, Y.L., et al., 2011. Identification of the nanogold particle-induced endoplasmic reticulum stress by omic techniques and system biology analysis. ACS Nano 5, 9354-9369.

Valant, J., Iavicoli, I., Drobne, D., 2012. The importance of a validated standard methodology to define in vitro toxicity of nano-TiO2. Protoplasma 249, 493-502.

Vandesompele, J., De Preter, K., Pattyn, F., et al., 2002. Accurate normalization of real-time quantitative RT-PCR data by geometric averaging of multiple internal control genes. Genome Biol. 3, Research0034.

Wang, W.M., Deng, M.J., Liu, X.T., et al. TLR4 Activation Induces Nontolerant Inflammatory Response in Endothelial Cells. Inflammation 34, 509-518.

Weir, A., Westerhoff, P., Fabricius, L., et al., 2012. Titanium Dioxide Nanoparticles in Food and Personal Care Products. Environ. Sci. Technol. 46, 2242-2250.

Xia, T., Li, N., Nel, A.E., 2009. Potential Health Impact of Nanoparticles. Annu. Rev. Public Health 30, 137-150.

Zhang, R., Piao, M.J., Kim, K.C., et al., 2012. Endoplasmic reticulum stressis involved in silver nanoparticles-induced apoptosis. Int. J. Biochem. Cel. Biol. 44, 224-232.

Zucker, R.M., Massaro, E.J., Sanders, K.M., et al., 2010. Detection of TiO2 Nanoparticles in Cells by Flow Cytometry. Cytometry A 77A, 677-685.

TABLES

Table 1. Comparison of Z-potential values (mV) in different media.

Medium / Specimen	H_2O	PBS+BSA	RPMI 1640	EBM2
Co_3O_4	-19.08 ± 1.15	-7.85 ± 1.97	-8.20 ± 1.37	-4.70 ± 3.57
TiO_2	-31.74 ± 1.02	-13.05 ± 2.13	-3.63 ± 1.07	+9.8 ±2.44

Mean values ± SD.

Table 2. Expression of adhesion molecules

HAEC Cells	Times / NPs	4 h	8 h	12 h	24 h
ICAM	Co_3O_4	2.51 ± 0.05^b	2.86 ± 0.15^b	1.83 ± 0.07^b	$0,71 \pm 0.12$
	TiO_2	1.27 ± 0.08	3.55 ± 0.59^c	3.1 ± 0.08^c	2.09 ± 0.07
VCAM	Co_3O_4	4.45 ± 1.66^a	8.31 ± 2.90^b	1.04 ± 0.29	0.23 ± 0.03
	TiO_2	0.96 ± 0.27	7.15 ± 2.05^b	3.52 ± 0.89	2.88 ± 0.33
SELE	Co_3O_4	5.63 ± 2.54^b	4.29 ± 0.08^b	$0.37 \pm 0,07$	0.21 ± 0.11
	TiO_2	5.33 ± 1.17^b	13.93 ± 4.54^c	8.28 ± 0.84^b	2.31 ± 1.23

HUVEC Cells	Times / NPs	4 h	8 h	12 h	24 h
ICAM	Co_3O_4	3.16 ± 0.12^c	1.96 ± 0.04	0.93 ± 0.11	1.16 ± 0.06
	TiO_2	2.12 ± 0.16	2.05 ± 0.05	1.45 ± 0.06	1.33 ± 0.15
VCAM	Co_3O_4	2.94 ± 0.25^b	0.81 ± 0.60	0.06 ± 0.01^a	0.02 ± 0.01^a
	TiO_2	3.43 ± 0.95^b	2.06 ± 0.57^a	0.66 ± 0.41	0.05 ± 0.01^a
SELE	Co_3O_4	1.63 ± 0.10^a	0.50 ± 0.16^a	ND	ND
	TiO_2	3.41 ± 0.80^c	1.93 ± 0.25^a	0.73 ± 0.25	0.62 ± 0.16

The values were compared with those observed in untreated controls. Statistical significance: $^a p < 0.05$; $^b p < 0.01$; $^c p < 0.001$

FIGURE LEGENDS

Figure 1: Characterisation of nanoparticles. TEM image of a cluster of agglomerated CoNPs (A) and a small cluster of a few TiNPs (B). Size distribution analysis of CoNPs (C) and TiNPs (D). Comparison of size distributions of CoNPs (E) and TiNPs (F) in different media (water, EBM2, PBS+BSA, RPMI 1640) obtained by means of DLS.

Figure 2: Cell interactions and uptake of NPs assessed by means of 24-hour flow cytometry. **A)** Flow cytometry analysis of side scatter (SSC) and forward scatter (FSC). Representative cytograms of unexposed cells (control) and cells exposed to 20 µg/mL for 30 min. **B)** Influence of incubation time on side scatter (SSC). The continuous lines correspond to HUVECs and the dashed lines to HAECs. Mean SSC ratio (treated/control) $\pm$ SD. Significant differences from controls: ^{a} $p < 0.05$; ^{b} $p < 0.01$; ^{c} $p < 0.001$.

Figure 3: Viability of cells exposed to 1-100 µg NPs/mL for 24 hours. Values normalised to controls (%). Mean values (± SD) of at least three separate experiments, each carried out in eight replicates. Significant differences from controls: ^{a} $p < 0.05$; ^{b} $p < 0.01$; ^{c} $p < 0.001$.

Figure 4: Monoparametric DNA analysis of cell cycle distribution after 24 hours' treatment with 20 µg NPs/mL. The three distinct phases (G0/G1, S and G2/M) in the proliferating cell population correspond to different peaks. Significant differences from controls: ^{a} $p < 0.05$; ^{b} $p < 0.01$; ^{c} $p < 0.001$.

Figure 5: Oxidative stress. ROS production (A), TBARS (B), glutathione levels (C) and HO-1 expression (D) during cell exposure to NPs. The values were related to the mean value of the corresponding control cells: (sample value/control value)x100. The columns represent the mean

values ± SD of three separate experiments, each carried out in triplicate. Significant differences from untreated controls: [a] $p < 0.05$; [b] $p < 0.01$; [c] $p < 0.001$.

Figure 6: Effect of NPs on cytokine release in HAECs and HUVECs. The concentrations in the culture medium were referred to controls (%). Significant differences from untreated cells: [a] $p < 0.05$; [b] $p < 0.01$; [c] $p < 0.001$.

Figure1

Click here to download high resolution image

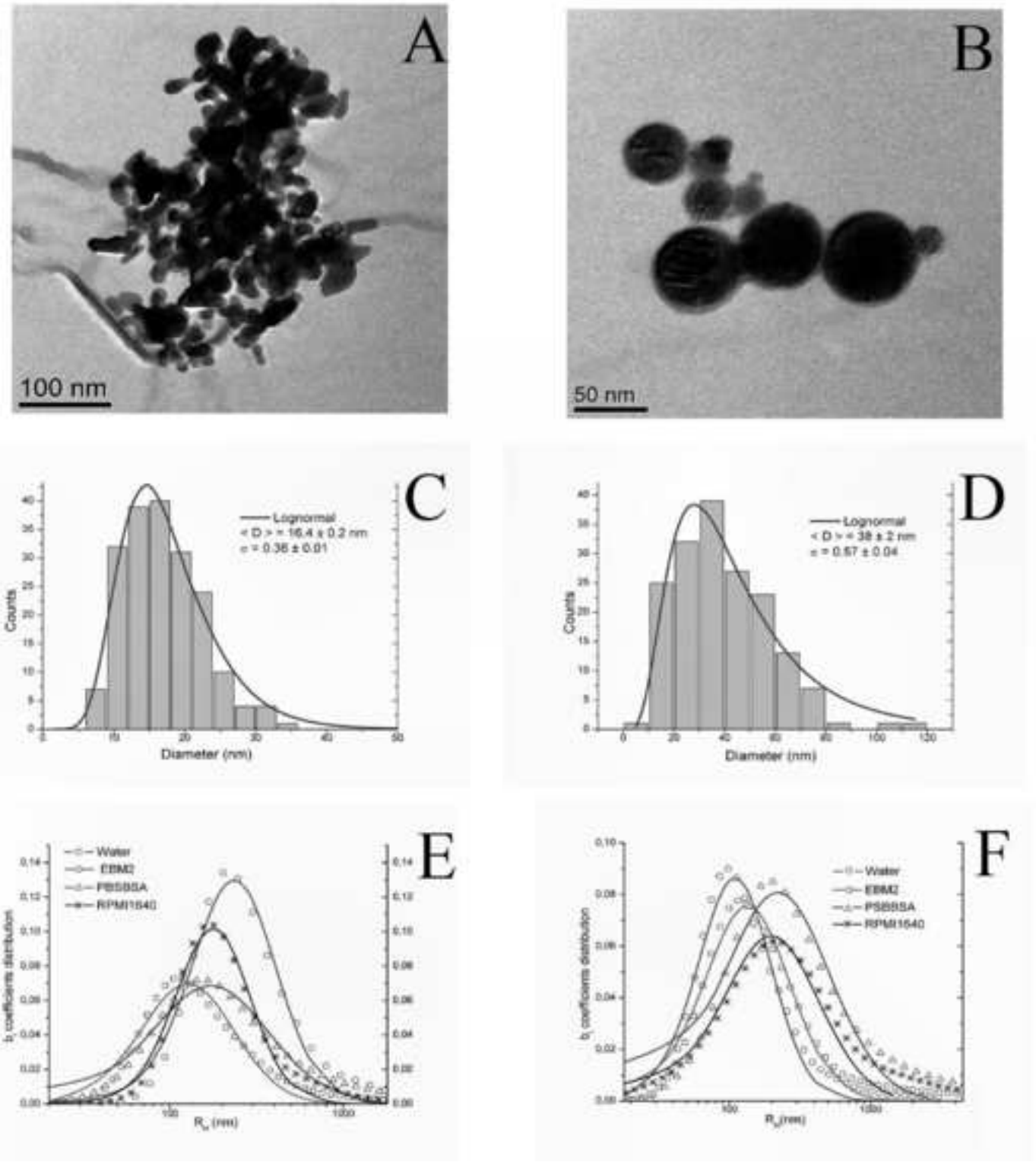

Figure2

Click here to download high resolution image

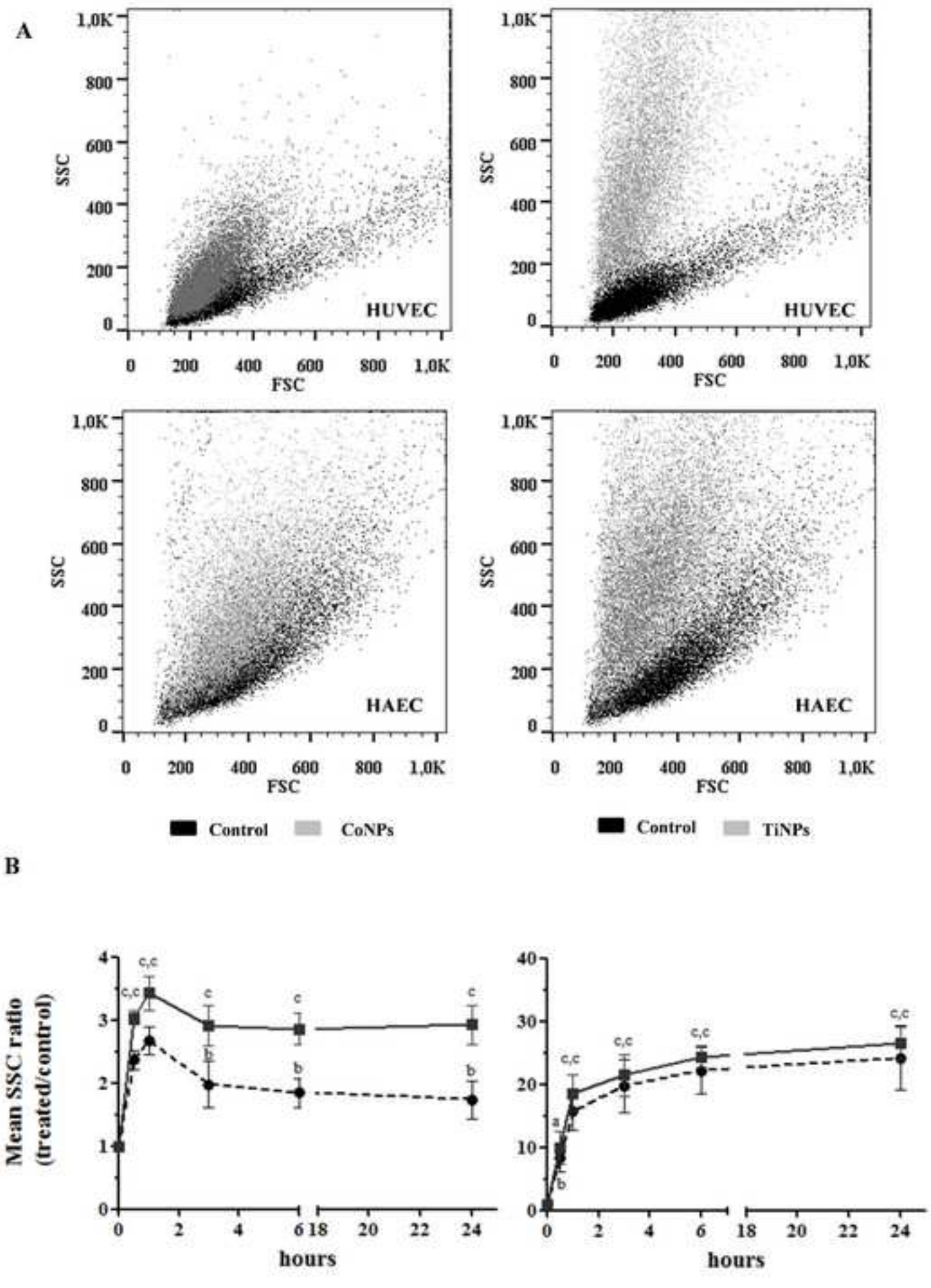

Figure3

Click here to download high resolution image

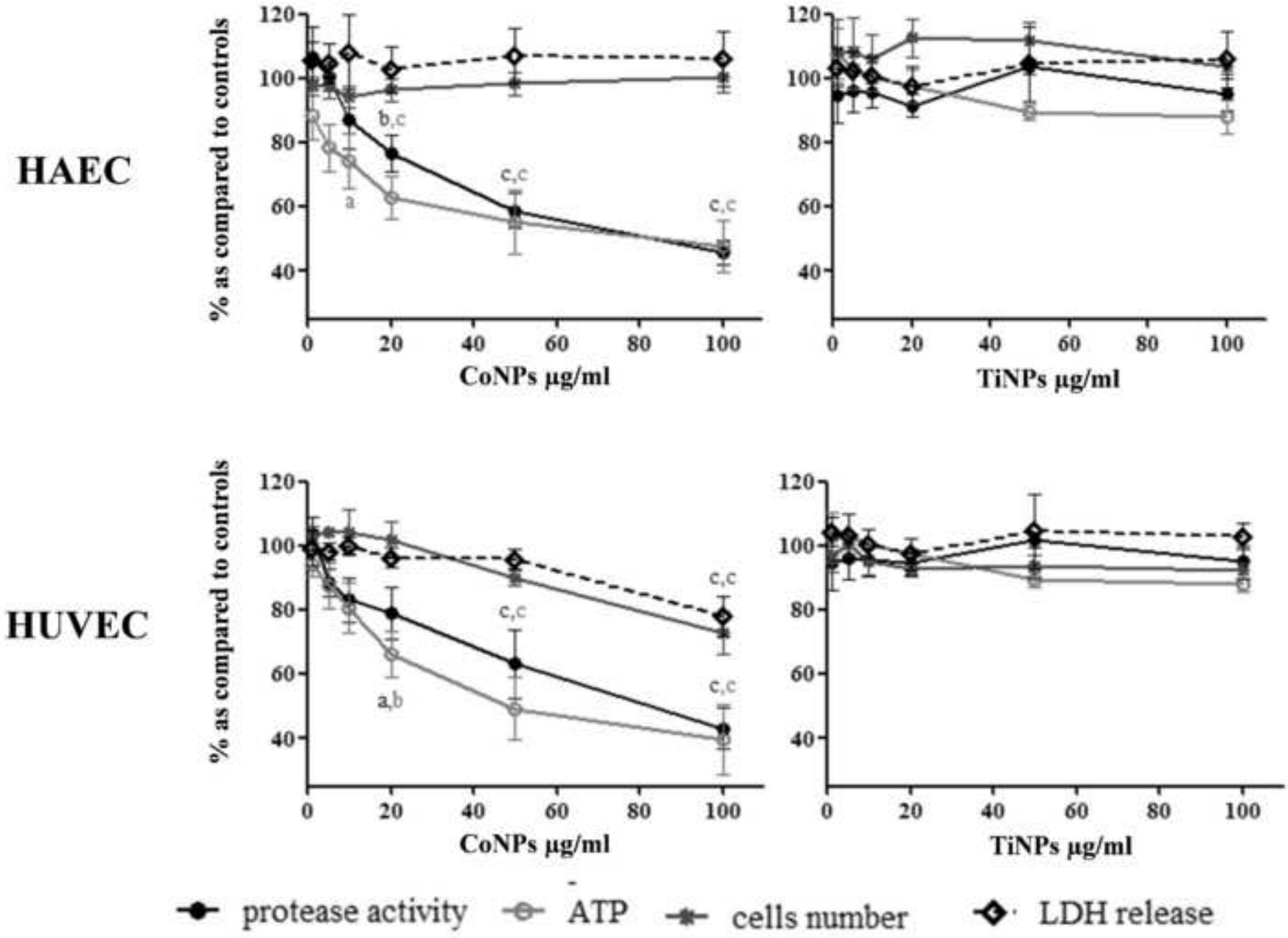

Figure4

Click here to download high resolution image

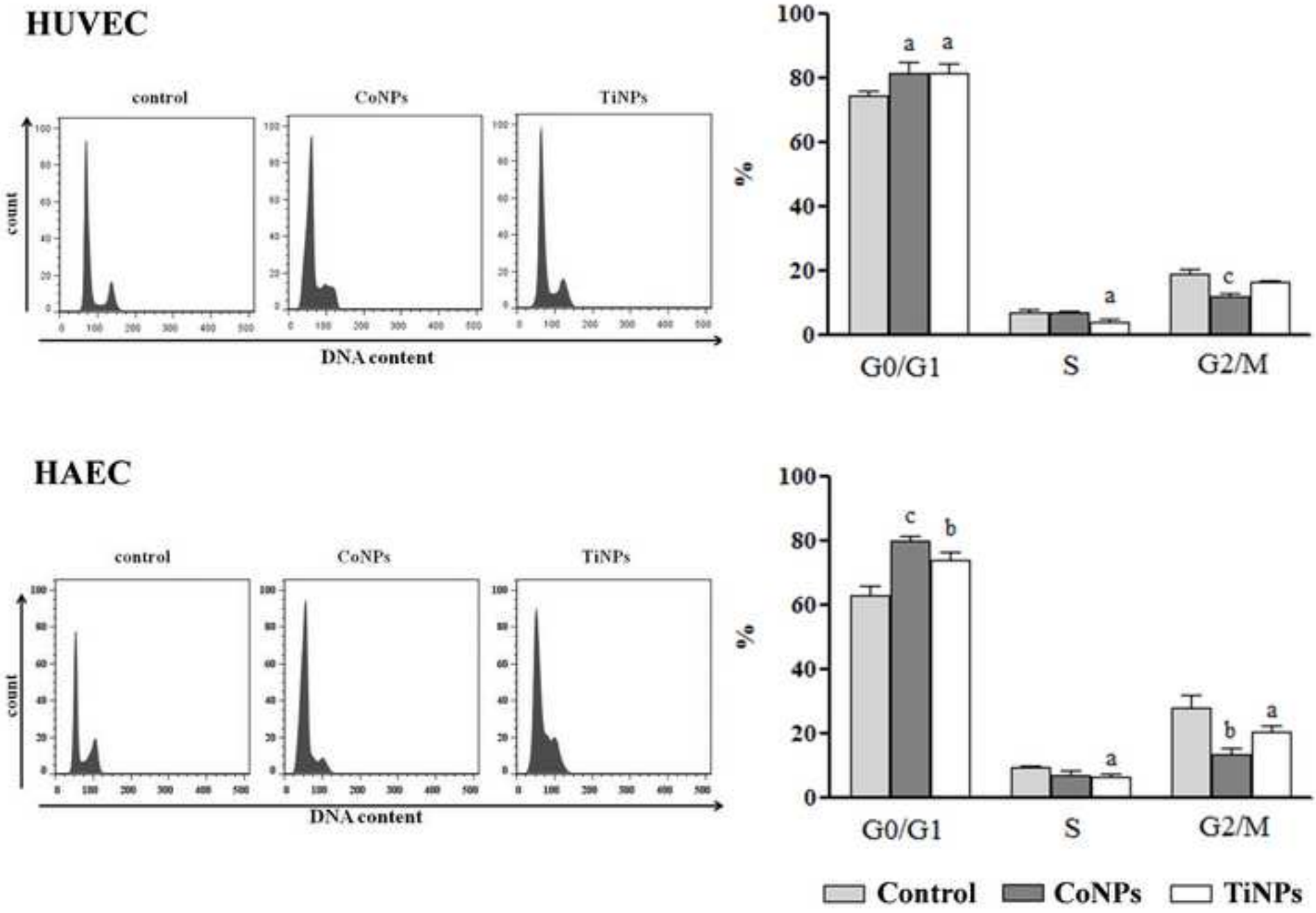

Figure5

Click here to download high resolution image

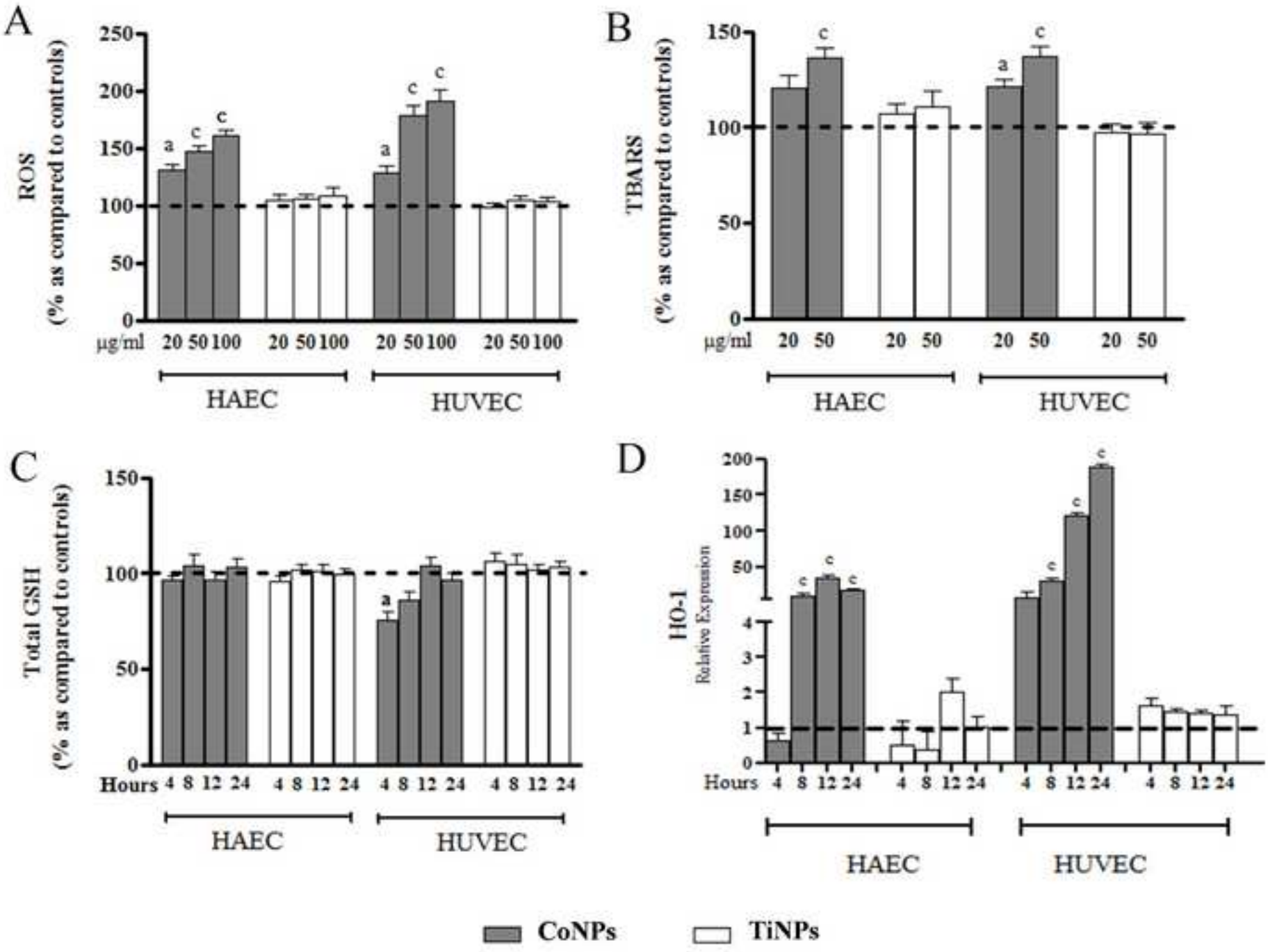

Figure6

Click here to download high resolution image

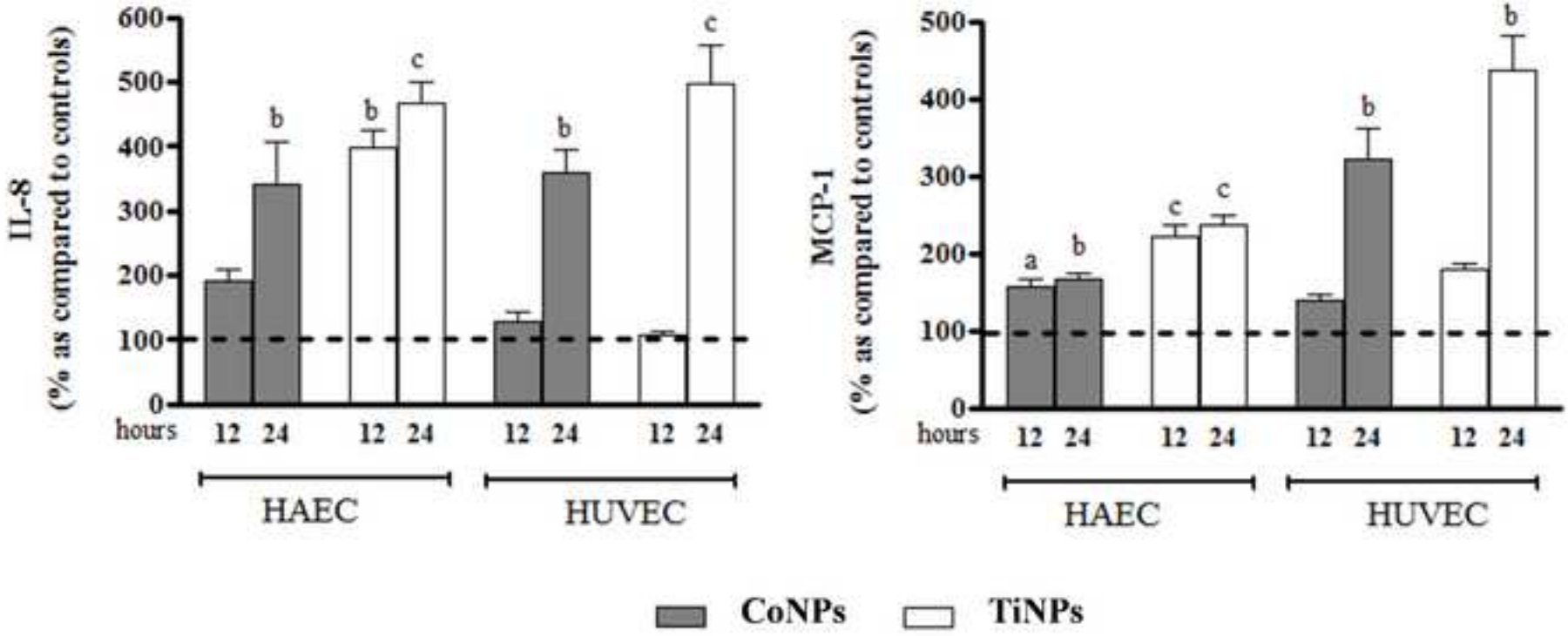

Graphical Abstract (for review)

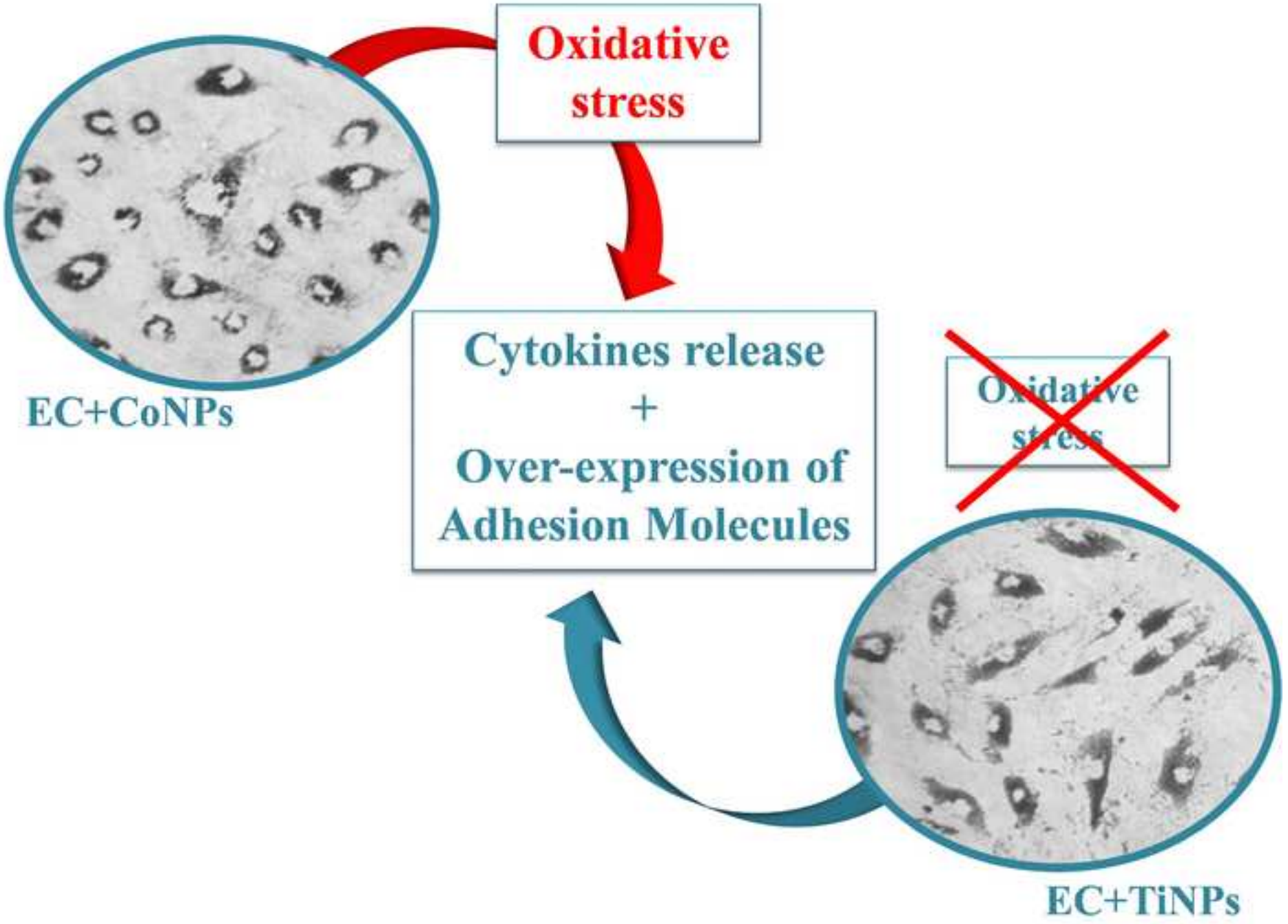

Highlights

- Endothelial cells (HAEC-HUVEC) were exposed to Co_3O_4 and TiO_2 Nanoparticles (NPs).
- CoNPs, but not TiNPs, caused metabolic impairment and oxidative stress.
- Both NPs induced over-expression of adhesion molecules and release of cytokines.
- Different vascular localization may explain heterogeneous cellular response.

Goldoni

Click here to download Conflict of Interest: goldoni.pdf

Alinovi

Click here to download Conflict of Interest: alinovi.pdf

Pinelli

Click here to download Conflict of Interest: pinelli.pdf

Campanini

Click here to download Conflict of Interest: campanini.pdf

Aliatis

Click here to download Conflict of Interest: aliatis.pdf

Bersani

Click here to download Conflict of Interest: bersani.pdf

Lottici

Click here to download Conflict of Interest: lottici.pdf

Iavicoli

Click here to download Conflict of Interest: iavicoli.pdf

Petyx

Click here to download Conflict of Interest: petyx.pdf

Mozzoni

Click here to download Conflict of Interest: mozzoni.pdf

Mutti

Click here to download Conflict of Interest: mutti.pdf